SI Appendix

Materials and Methods

Culture maintenance and experimental setup. All four strains of marine AOA were maintained in artificial seawater medium in the dark without shaking. *Nitrosopumilus maritimus* strain SCM1 was grown in HEPES-buffered Synthetic Crenarchaeota Medium (SCM) containing 1 mM NH_4Cl as described previously (1, 2). Strains HCA1, HCE1 and PS0 are three newly isolated *N. maritimus*-like marine AOA strains; they were isolated from a depth of 50 m water at the Puget Sound Regional Synthesis Model (PRISM) Station P10, a depth of 17 m water (nitrite maximum) at the PRISM Station P12, and Puget Sound surface sediment collected from a Seattle beach, respectively (3). These new isolates were defined as obligate mixotrophs and cultured in HEPES-buffered SCM supplemented with 500 μM NH_4Cl and 100 μM α-ketoglutaric acid (3). To investigate the influence of growth temperature on the membrane compositional regulation of marine AOA, early stationary phase cultures of strains SCM1, HCA1, HCE1 and PS0 (1ml) were inoculated into 100 ml growth medium and incubated in triplicate at temperatures ranging from 15 to 35˚C, 10 to 30˚C, 10 to 25 ˚C, and 25˚C, respectively. To assess the impact of O_2 concentration on membrane composition, strains SCM1 and PS0 were grown in triplicate at nine different O_2 concentrations, from 0.1% to 21% in the headspace. Briefly, experiments were carried out in 246 ml capacity serum bottles (Wheaton, NJ, USA) that contained 100ml of HEPES-buffered SCM supplemented with 100 μM NH_4Cl (10 micromoles NH_4Cl total). An organic supplement (100 μM α-ketoglutaric acid) was additionally added to medium used to culture strain PS0. The headspace of each bottle was sealed using air-tight butyl rubber septa and aluminum crimps (Wheaton). Atmospheric O_2 was removed by flushing bottle headspace

with N_2 through a sterile 0.22 µm Millex-GP syringe filter at > 50 ml/min for 10 min. The medium inside of the bottle was shaken well during the purge process. Subsequently, 0.04% (v/v) of high-purity CO_2 was injected back to exchange headspace N_2 in bottles. The appropriate amounts of high-purity O_2 were also injected back into each headspace to achieve 0.1%, 0.2%, 0.5%, 1%, 2%, 3%, 5%, 10%, and 21% O_2 (v/v). Initial O_2 concentration in the aqueous phase were calculated according to Henry`s law, approximately achieving 1, 2, 5, 11, 21, 32, 53, 106, 213 µM in the aqueous phase under equilibrium conditions. Headspace O_2 concentration of each bottle was measured and confirmed before each experiment using an SRI 8610SC gas chromatograph equipped with a thermal conductivity detector (SRI instruments, CA., USA). The initial amounts of O_2 present in the serum bottles varied from ~6 to ~1253 micromoles (corresponding to 0.1% to 21% of initial headspace O_2). Early stationary phase cultures of strains SCM1 and PS0 (1ml) were inoculated into each bottle and incubated at 30˚C and 26˚C, respectively. Growth was routinely monitored by sampling and measuring nitrite production as described previously (3). All experiments were conducted in SCM buffered with 10mM HEPES, which is sufficient to maintain culture pH with as much as 2.5mM nitrite production. Since no more than 1mM nitrite was produced in any of the growth experiments, there was no appreciable change in pH among culture treatments and between the beginning and end of each growth experiment. The final cell densities were determined by microscopic counts of SybrGreen-stained cells (Invitrogen, Carlsbad, USA) as previously described (3). Early stationary phase cells were harvested on 0.22 µm Durapore membrane filters (Millipore Co., MA, U.S.) and stored at -20˚C until acid hydrolysis.

Lipid extraction and analysis. Durapore membrane filters containing the cultured cells were handled according to Huguet et al., (2010) (4). Briefly, filters were placed in Teflon vials, flushed with N_2, and hydrolyzed with 5% HCl in methanol (v/v) for 4 hours at 70˚C. After heating, the methanol was transferred to a combusted glass vial and equal parts dichloromethane (DCM) and MilliQ were added to separate the phases. The DCM fraction, containing GDGTs with polar head groups removed during the hydrolysis step, was collected and transferred to a second combusted glass vial. The remaining acid solution was extracted 3 additional times with DCM, and the DCM extracts were combined. The DCM extract was rinsed at least six times with water to remove any remaining acid. The extracts were dried under N_2 before analysis using HPLC/MS. A known amount of the internal quantification standard, C_{46} GDGT, was added to all dried extracts (5). The samples with internal standard were re-dissolved in 1% isopropanol in hexane (v/v) before injection on the HPLC/MS. Lipid analysis was done using atmospheric pressure chemical ionization (APCI) on an Agilent 1100 Series liquid chromatograph coupled to an Agilent ion trap (XCT) mass spectrometer (LC-MS) according to Hopmans et al., (2000) (6). Separation of the core GDGTs was achieved on an Alltech Prevail Cyano column (2.1 × 150 mm, 3 µm) maintained at 30˚C. The column was fitted with a Prevail Cyano guard column (7.5 × 4.6 mm, 5 µm). Core GDGTs were eluted with 99:1 hexane to isopropanol (solvent A) and 90:10 hexane to isopropanol (solvent B) at a flow rate of 0.2 ml min^{-1}. Solvent A was run isocratically from 0 to 5 min, followed by a linear gradient of 0 to 8.2% solvent B over the next 40 min. The column was cleaned by back flushing with 100% solvent B for 8 min and then equilibrated back to 100% solvent A for 10 min. Detection was achieved using APCI in positive mode with the following conditions: nebulizer pressure of 60 psi, vaporizer temperature of 400˚C, nitrogen drying gas flow of 6 l min^{-1} at 200˚C, capillary

voltage of -3.5 kV, and corona of 4 μA. The scanning mass range was 730–1350 m/z. Triplicate filters from the same culture treatment were analyzed and each filter sample was injected onto the LC-MS at least 2 times. Absolute lipid concentrations were calculated by comparison of each GDGT peak area with the peak area of the C_{46} internal standard. The relative abundance (%) of each GDGT was calculated by dividing the peak area of each lipid by the sum of the peak areas of all the core GDGTs.

1. Könneke M*, et al.* (2005) Isolation of an autotrophic ammonia-oxidizing marine archaeon. *Nature* 437(7058):543-546.
2. Martens-Habbena W, Berube PM, Urakawa H, de la Torre JR, & Stahl DA (2009) Ammonia oxidation kinetics determine niche separation of nitrifying Archaea and Bacteria. *Nature* 461(7266):976-U234.
3. Qin W*, et al.* (2014) Marine ammonia-oxidizing archaeal isolates display obligate mixotrophy and wide ecotypic variation. *Proc Natl Acad Sci USA* 111(34):12504-12509.
4. Huguet C, Martens-Habbena W, Urakawa H, Stahl DA, & Ingalls AE (2010) Comparison of extraction methods for quantitative analysis of core and intact polar glycerol dialkyl glycerol tetraethers (GDGTs) in environmental samples. *Limnol Oceanogr Methods* 8(4):127-145.
5. Huguet C*, et al.* (2006) An improved method to determine the absolute abundance of glycerol dibiphytanyl glycerol tetraether lipids. *Org Geochem* 37(9):1036-1041.
6. Hopmans EC, Schouten S, Pancost RD, van der Meer MTJ, & Damsté JSS (2000) Analysis of intact tetraether lipids in archaeal cell material and sediments by high performance liquid chromatography/atmospheric pressure chemical ionization mass spectrometry. *Rapid Commun Mass Spectrom* 14(7):585-589.

Figure S1.

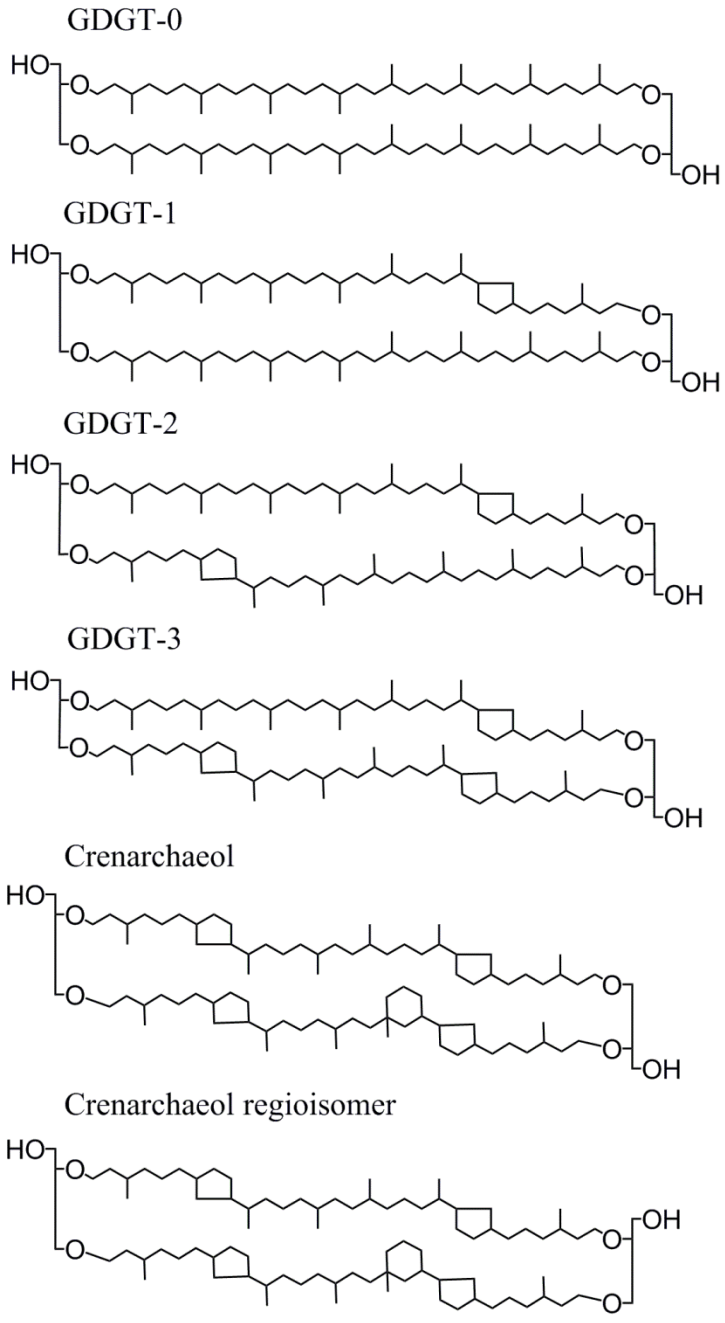

Figure S1. Structures of the glycerol dibiphytanyl glycerol tetraethers (GDGTs) core lipids of marine AOA.

Figure S2.

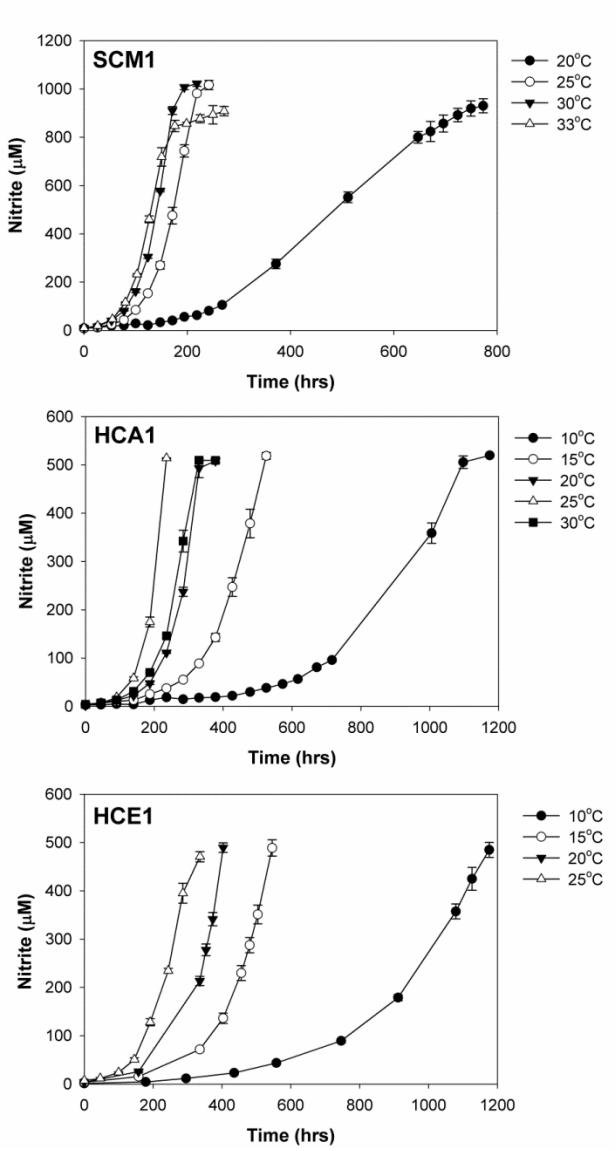

Figure S2. Effects of temperature on the ammonia oxidation activities of strains SCM1, HCA1 and HCE1. Early stationary phase cultures (1% inoculum) were transferred to the growth medium supplemented with 1mM NH_4Cl (strain SCM1) or 500 μM NH_4Cl (strains HCA1 and HCE1). Ammonia oxidation activity was indicated by nitrite accumulation over time. Early stationary phase cells were harvested for the lipid analysis. Error bars represent the SD of data from triplicate cultures.

Figure S3.

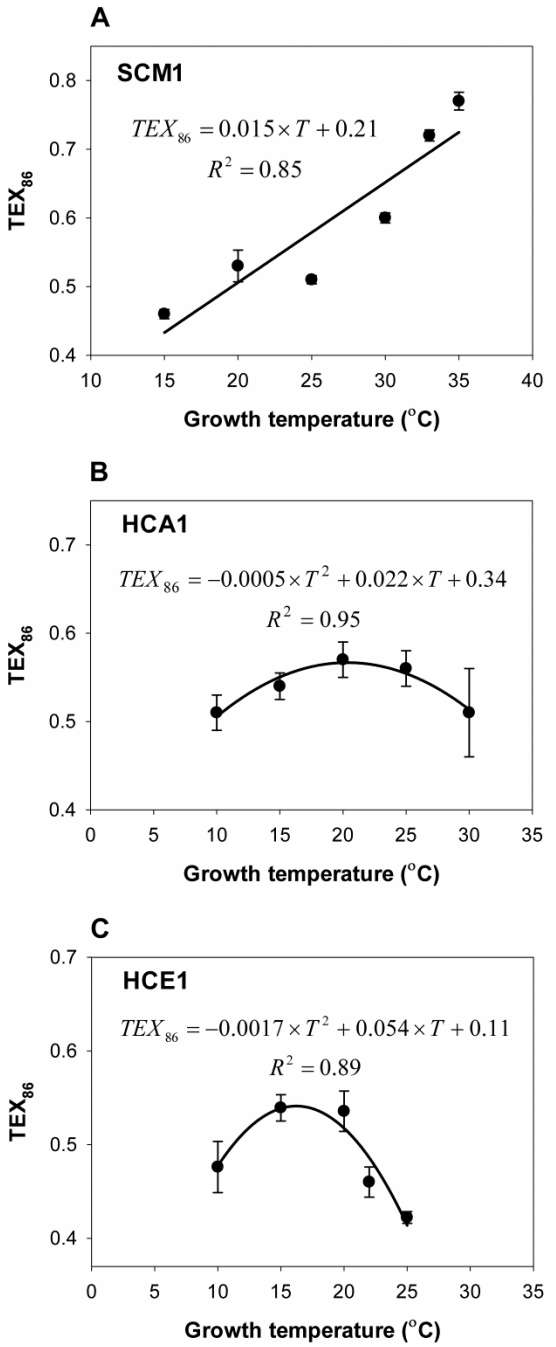

Figure S3. Correlations of TEX_{86} values with growth temperatures of strains SCM1 (*A*), HCA1 (*B*) and HCE1 (*C*). Error bars represent the SD of data from triplicate cultures.

Figure S4.

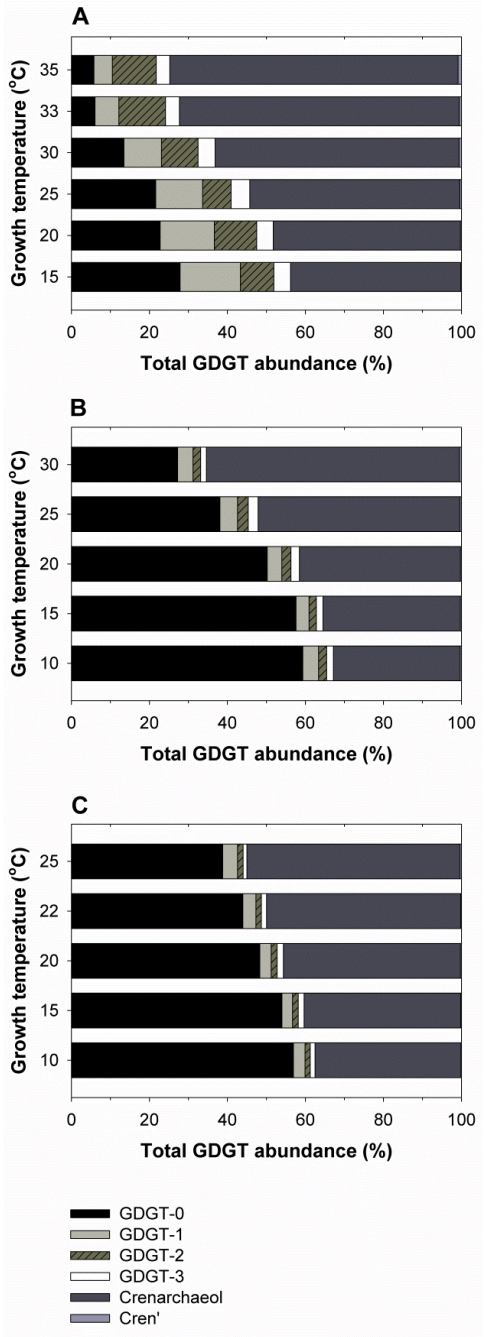

Figure S4. Relative abundances of GDGTs in total cellular lipids of marine AOA strains SCM1 (*A*), HCA1 (*B*) and HCE1 (*C*) at different temperatures.

Figure S5.

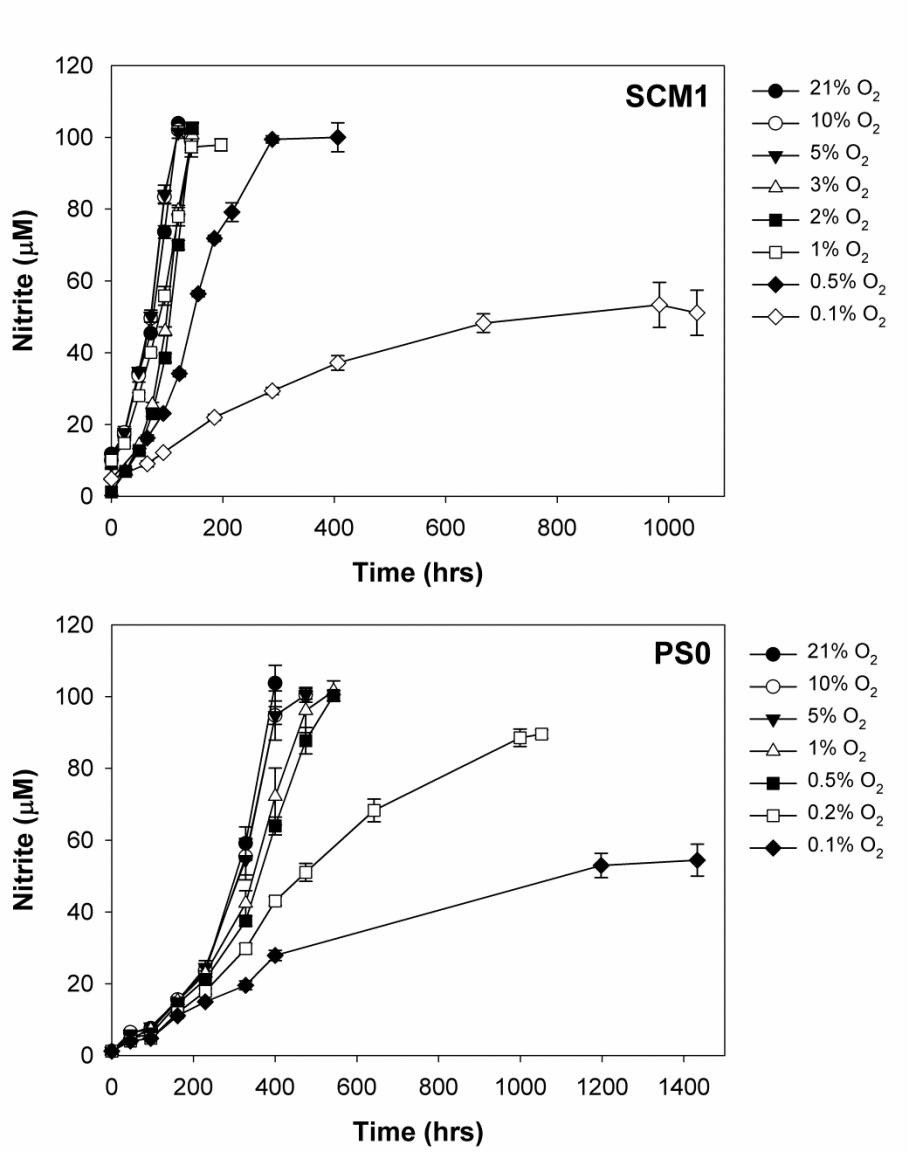

Figure S5. Effects of O_2 concentration on the ammonia oxidation activities of strains SCM1 and PS0. Early stationary phase cultures (1% inoculum) were transferred to the growth medium supplemented with 100 μM NH_4Cl for both strains SCM1 and PS0. Early stationary phase cells were harvested for the lipid analysis. Error bars represent the SD of data from triplicate cultures.

Figure S6.

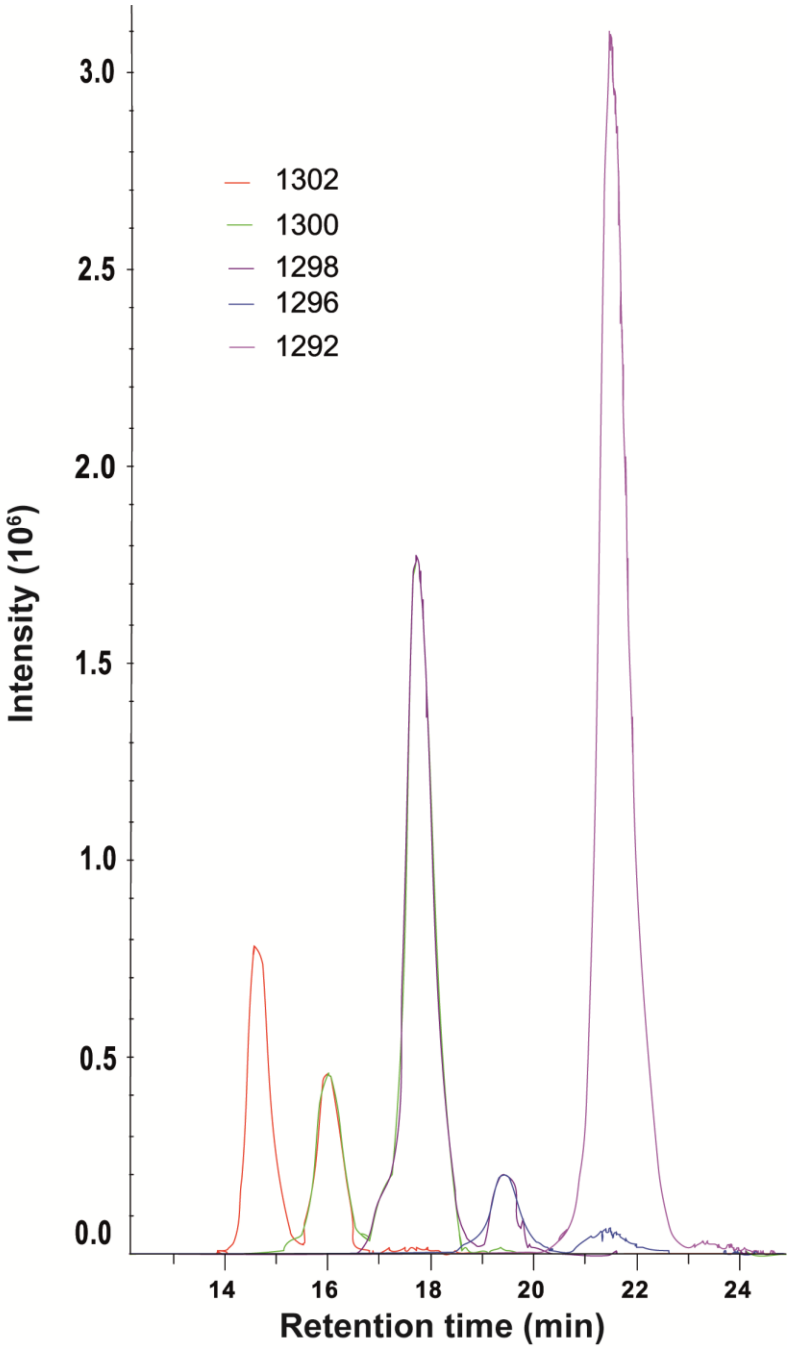

Figure S6. HPLC/MS base peak chromatogram showing the distribution of GDGT-0 (*m/z* 1302), GDGT-1 (*m/z* 1300), GDGT-2 (*m/z* 1298), GDGT-3 (*m/z* 1296), crenarchaeol and crenarchaeol regioisomer (*m/z* 1292) of marine AOA grown at 0.1% initial headspace O_2.

Figure S7.

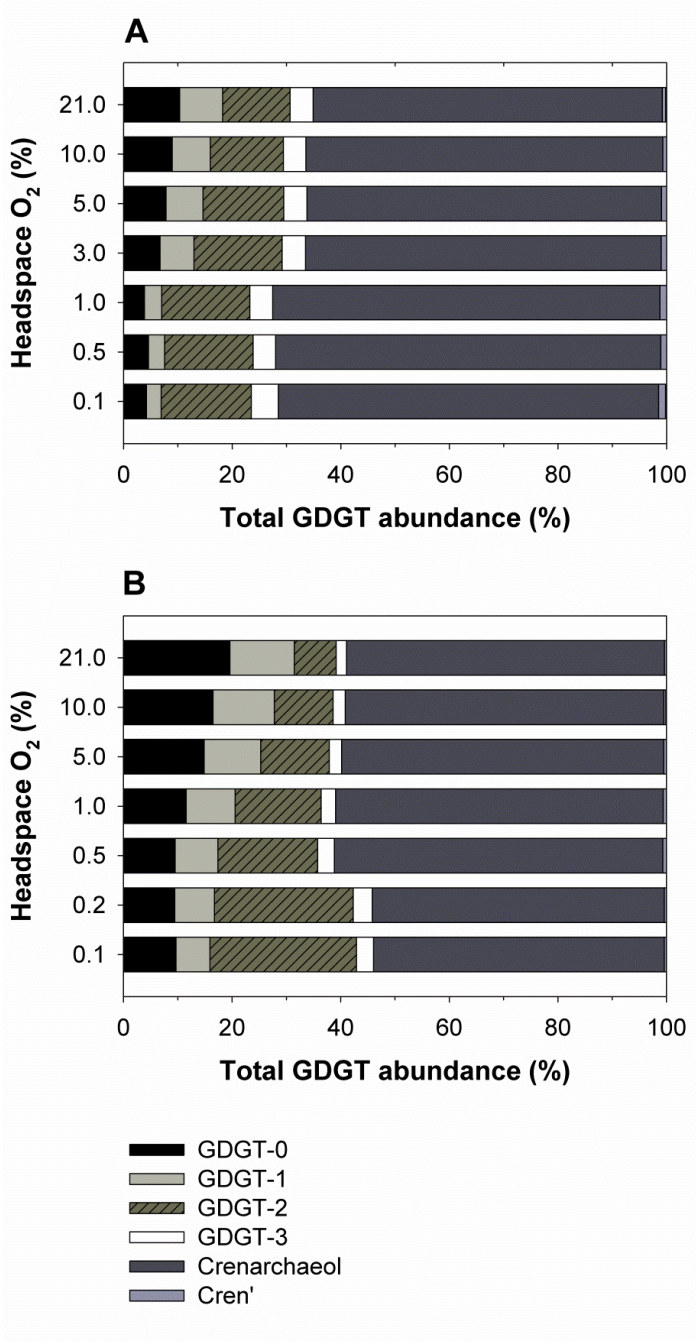

Figure S7. Relative abundances of GDGTs in total cellular lipids of marine AOA strains SCM1 (*A*) and PS0 (*B*) with different initial headspace O_2 concentrations.

Table S1. Cell densities, lipid contents and TEX_{86} values of different marine AOA strains grown at selected temperatures

Strain	Growth temperature (°C)	Cell density at early stationary phase (ml^{-1})	Total GDGTs ($fg\ cell^{-1}$)	TEX_{86}
SCM1	15	–	–	0.46
	20	7.27×10^{7}	2.00	0.53
	25	8.10×10^{7}	2.22	0.51
	30	8.35×10^{7}	2.02	0.60
	35	–	–	0.77
HCA1	10	–	–	0.51
	15	3.82×10^{7}	2.05	0.54
	20	3.87×10^{7}	2.09	0.57
	25	3.49×10^{7}	1.76	0.56
	30	3.65×10^{7}	2.27	0.51
HCE1	15	3.69×10^{7}	1.53	0.54
	20	3.70×10^{7}	1.41	0.54
	25	–	–	0.42
PS0	25	3.59×10^{7}	3.01	0.38

Table S2. Relative abundances of GDGTs in total cellular lipids and ring index values of marine AOA isolates grown at selected temperatures

Strain	Growth temperature (˚C)	Relative abundance of GDGTs (%)						Ring index
		0	1	2	3	Cren	Cren'	
SCM1	15	27.86	15.47	8.57	4.28	43.67	0.15	2.65
	20	22.76	13.91	10.84	4.26	47.99	0.24	2.90
	25	21.62	12.02	7.32	4.76	53.91	0.37	3.12
	30	13.47	9.63	9.37	4.37	62.58	0.58	3.57
	33	6.04	6.14	11.97	3.56	71.73	0.56	4.02
	35	5.78	4.71	11.26	3.49	73.91	0.84	4.11
HCA1	10	59.34	4.04	2.09	1.71	32.51	0.31	1.77
	15	57.60	3.34	1.88	1.71	35.17	0.30	1.90
	20	50.22	3.73	2.37	2.15	41.27	0.26	2.23
	25	38.09	4.52	2.71	2.54	51.78	0.36	2.78
	30	27.23	3.95	1.97	1.45	64.90	0.50	3.39
HCE1	10	56.92	2.98	1.34	1.25	37.39	0.12	1.97
	15	53.99	2.71	1.46	1.50	40.14	0.20	2.12
	20	48.33	2.90	1.53	1.58	45.42	0.23	2.39
	22	43.96	3.36	1.41	1.32	49.78	0.17	2.60
	25	38.81	3.78	1.46	0.96	54.65	0.34	2.85
PS0	25	25.33	12.59	5.53	1.83	54.41	0.31	3.03

Table S3. Cell densities, O_2 utilization and TEX_{86} values of marine AOA strains grown at selected initial headspace O_2 concentrations

Strain	Initial headspace O_2	Initial amount of O_2 (micromole)	Residual amount of O_2 (micromole)	Initial Cell density (ml^{-1})	Cell density at early stationary phase (ml^{-1})	TEX_{86}
SCM1	0.1%	6.0	0	2.83×10^5	4.0×10^6	0.89
	0.5%	29.8	14.8	2.72×10^5	6.3×10^6	0.88
	1%	59.7	44.7	2.78×10^5	6.6×10^6	0.87
	5%	298.3	283.3	2.88×10^5	6.8×10^6	0.74
	10%	596.5	581.5	2.77×10^5	6.9×10^6	0.72
	21%	1252.7	1237.7	2.83×10^5	7.9×10^6	0.68
PS0	0.2%	11.9	0	2.51×10^5	6.7×10^6*	0.80
	0.5%	29.8	14.8	2.33×10^5	7.0×10^6	0.74
	1%	59.7	44.7	2.95×10^5	7.0×10^6	0.68
	5%	298.3	283.3	$2.88.\times10^5$	6.8×10^6	0.59
	10%	596.5	581.5	$2.43.\times10^5$	6.8×10^6	0.55
	21%	1252.7	1237.7	$2.70.\times10^5$	6.7×10^6	0.45

*The slightly higher cell densities than predicted from ammonia oxidation may reflect some variation in the incorporation of α-ketoglutarate into cellular biomass under low O_2.

Table S4. Relative abundances of GDGTs in total cellular lipids and ring index values of strains SCM1 and PS0 grown at selected initial headspace O_2 concentrations

Strain	Initial headspace O_2	Relative abundance of GDGTs (%)						Ring index
		0	1	2	3	Cren	Cren'	
SCM1	0.1%	4.21	2.70	16.60	4.99	70.03	1.28	4.08
	1%	3.84	3.17	16.26	4.19	71.35	1.18	4.11
	5%	7.81	6.84	14.84	4.3	65.28	0.89	3.80
	10%	8.95	7.04	13.43	4.16	65.72	0.62	3.78
	21%	10.32	7.93	12.42	4.26	64.28	0.61	3.71
PS0	0.1%	9.69	6.24	27.00	3.14	53.53	0.37	3.39
	0.2%	9.44	7.31	25.58	3.48	53.78	0.36	3.40
	0.5%	9.50	7.90	18.37	3.06	60.49	0.64	3.60
	1%	11.57	9.00	15.82	2.69	60.33	0.55	3.53
	5%	14.84	10.45	12.62	2.26	59.34	0.43	3.42
	10%	16.49	11.30	10.81	2.22	58.70	0.39	3.35
	21%	19.58	11.89	7.69	1.94	58.53	0.29	3.27